



Observation of spontaneous ferromagnetism in a two-dimensional electron system

M. S. Hossain^a , M. K. Ma^a, K. A. Villegas Rosales^a , Y. J. Chung^a , L. N. Pfeiffer^{a,1}, K. W. West^a, K. W. Baldwin^a, and M. Shayegan^{a,1}

^aDepartment of Electrical Engineering, Princeton University, Princeton, NJ 08544

Contributed by L. N. Pfeiffer, November 3, 2020 (sent for review August 28, 2020; reviewed by David Ceperley, Steven A. Kivelson, and Myriam P. Sarachik)

What are the ground states of an interacting, low-density electron system? In the absence of disorder, it has long been expected that as the electron density is lowered, the exchange energy gained by aligning the electron spins should exceed the enhancement in the kinetic (Fermi) energy, leading to a (Bloch) ferromagnetic transition. At even lower densities, another transition to a (Wigner) solid, an ordered array of electrons, should occur. Experimental access to these regimes, however, has been limited because of the absence of a material platform that supports an electron system with very high quality (low disorder) and low density simultaneously. Here we explore the ground states of interacting electrons in an exceptionally clean, two-dimensional electron system confined to a modulation-doped AlAs quantum well. The large electron effective mass in this system allows us to reach very large values of the interaction parameter r_s , defined as the ratio of the Coulomb to Fermi energies. As we lower the electron density via gate bias, we find a sequence of phases, qualitatively consistent with the above scenario: a paramagnetic phase at large densities, a spontaneous transition to a ferromagnetic state when r_s surpasses 35, and then a phase with strongly nonlinear current-voltage characteristics, suggestive of a pinned Wigner solid, when r_s exceeds ≈ 38 . However, our sample makes a transition to an insulating state at $r_s \approx 27$, preceding the onset of the spontaneous ferromagnetism, implying that besides interaction, the role of disorder must also be taken into account in understanding the different phases of a realistic dilute electron system.

2D electron system | ferromagnetism | magnetotransport | metal-insulator transition | Wigner solid

The ground state of an interacting, dilute electron system and its magnetic properties have long been topics of great interest in many-body physics (1–7). At low densities the interaction energy dominates over the kinetic energy. A disorder-free, itinerant electron system at sufficiently low electron densities is expected to make a transition to a ferromagnetic ground state (1), namely, a Bloch ferromagnet. At even lower densities, electrons are predicted to condense into a Wigner solid, an ordered array of electrons (2). For a quantitative description, it is convenient to characterize the interacting electron system with the dimensionless parameter r_s , the average interelectron distance in units of the effective Bohr radius (equivalently, r_s is also the ratio of the Coulomb to Fermi energies). In a three-dimensional (3D) metal, r_s values are typically well below those required for the ferromagnetic transition (4). For a 2D electron system (2DES), Monte Carlo calculations (6) predict a transition to full magnetization when r_s exceeds 26, followed by another transition to a Wigner crystal state for $r_s > 35$. (These predictions are not all corroborated by other Monte Carlo calculations; see, e.g., ref. 7.) Achieving a very dilute and clean 2DES so that interaction phenomena are not hindered by disorder and single-particle localization, however, is extremely challenging. For a 2DES, we have $r_s = (me^2/4\pi\hbar^2\varepsilon\varepsilon_0)/(\pi n)^{1/2}$, where m is the electron band effective mass (in units of the free electron mass), ε is the dielectric constant, and n is the 2DES density. For

example, in a GaAs 2DES ($m = 0.067$ and $\varepsilon = 13$), $r_s \approx 26$ corresponds to a density of $n = 4.6 \times 10^8 \text{ cm}^{-2}$, which is indeed very difficult to attain (8, 9). In GaAs 2D hole systems ($m \approx 0.4$), large r_s values can be reached more easily, and in fact, hints of a Wigner solid formation near $r_s \approx 35$ were reported (10). However, partly because of the strong spin-orbit interaction, the extraction of spin polarization of 2D holes is not straightforward (11–13).

There are other semiconductor 2DEEs with large m , e.g., at a Si/SiO₂ or MgZnO/ZnO interface or in AlAs quantum wells, where large r_s values can be reached (14–23). Indeed, the spin polarization of interacting 2DEEs became a subject of intense interest and controversy in the context of the enigmatic metal-insulator transition (MIT) in dilute 2D carrier systems. Numerous experiments revealed that the spin/valley polarization in 2D carrier systems plays a role in the temperature dependence of conductivity (9, 11–22). In Si/SiO₂ 2DEEs, there were also claims that the spin susceptibility diverges at $r_s \approx 9$ and that the divergence coincides with the MIT (15, 16). However, these conclusions were not corroborated in measurements on a nearly ideal (single-valley, isotropic, very thin) 2DES confined to a narrow (4.5-nm-wide) AlAs quantum well (17). The AlAs data showed that the spin susceptibility does not diverge up to the highest experimentally achieved r_s (≈ 10). Instead, it closely follows the Monte Carlo calculations' results (6) and remains finite as the 2DES goes through the MIT at $r_s \approx 8$ (17). In very recent

Significance

Ground states of low-disorder, interacting, dilute electron systems are of fundamental interest in understanding electron-electron interaction phenomena. Our experimental data on a clean two-dimensional electron system reveal a sequence of transitions as the density is lowered. Starting from high densities, we observe a transition from a metallic state to an exotic insulating phase that is stabilized by disorder and interaction. As we further lower the density, we observe signs of a spontaneous transition to a ferromagnetic ground state and then to a strongly insulating state whose characteristics suggest that it is a pinned solid phase, possibly a (ferromagnetic) Wigner solid. We also find that the onset of ferromagnetism can be controlled by tuning the electrons' valley degree of freedom.

Author contributions: M.S.H. designed research; M.S.H. performed research; M.K.M., K.A.V.R., Y.J.C., L.N.P., K.W.W., K.W.B., and M.S. contributed new reagents/analytic tools; M.S.H. analyzed data; M.K.M. and K.A.V.R. helped with the measurements; and M.S.H. and M.S. wrote the paper.

Reviewers: D.C., University of Illinois at Urbana-Champaign; S.A.K., Stanford University; and M.P.S., The City College of the City University of New York.

The authors declare no competing interest.

Published under the [PNAS license](#).

See [online](#) for related content such as Commentaries.

¹To whom correspondence may be addressed. Email: loren@princeton.edu or shayegan@princeton.edu.

This article contains supporting information online at <https://www.pnas.org/lookup/suppl/doi:10.1073/pnas.2018248117/DCSupplemental>.

First published December 3, 2020.

studies which revisited the MIT problem in Si/SiO₂ 2DESs (21, 22), it was also concluded that there is no divergence of the spin susceptibility, even at densities lower than those reached in refs. 15, 16. Therefore, there has been no experimental evidence for a transition to full spin polarization in a 2DES at zero magnetic field prior to this work.

Experimental Results

We report here the observation of a spontaneous transition to a fully magnetized ground state and experimentally construct a comprehensive ground-state phase diagram for the interacting 2DES as a function of electron density (and r_s), as summarized in Fig. 1A. Our material platform is a very low disorder, dilute 2DES confined to a modulation-doped, 21-nm-wide AlAs quantum well ($\varepsilon = 10$) (24). The 2D electrons in our sample

occupy two in-plane conduction-band valleys with longitudinal and transverse effective masses $m_l = 1.1$ and $m_t = 0.20$, leading to an effective in-plane band mass m equal to $(m_l m_t)^{1/2} = 0.46$ (25). We refer to these valleys, whose electron occupancy we can control via the application of in-plane, uniaxial strain, by the direction of their major axis in the plane, [100] and [010] (SI Appendix, section I). The large effective mass, combined with the exceptionally high purity of the samples, allows us to achieve very large values of r_s while maintaining a strongly interacting system. This is evinced by our observation of signatures of fractional quantum Hall states in a perpendicular magnetic field a at density as low as $n = 1.20$ ($r_s \approx 45$) (see, e.g., Fig. 2 for data at $n = 1.70$ and relevant discussion); throughout the manuscript, we give the 2DES densities in units of 10^{10} cm⁻².

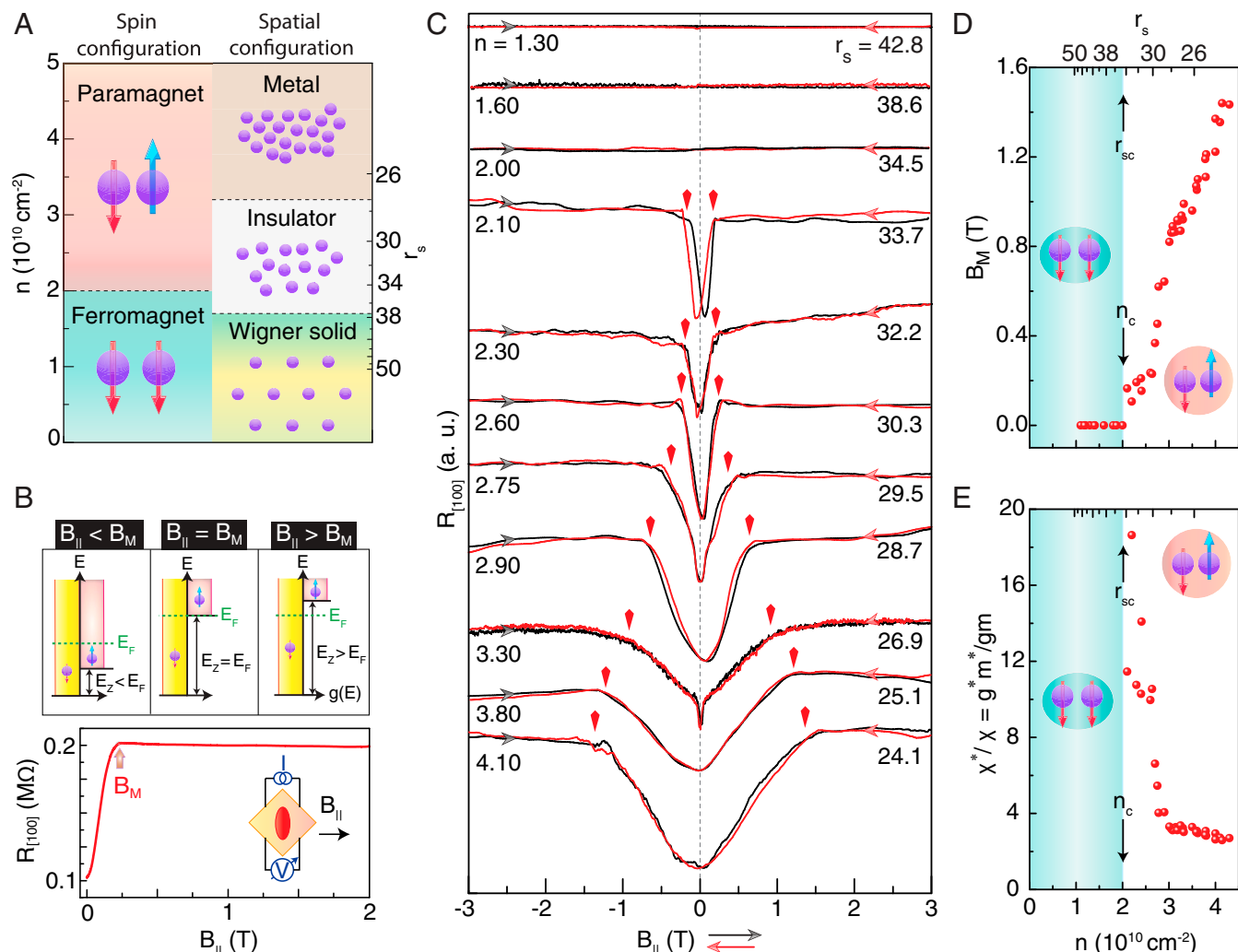


Fig. 1. Highlights of our experimental findings. (A) An experimental phase diagram, suggested by our study, for the ground states of an interacting 2DES at zero magnetic field as it is made progressively more dilute. The sample is paramagnetic at high densities, and its resistance vs. temperature dependence switches from metallic to insulating below a density of 3.2 (in units of 10^{10} cm⁻²). As the density is further lowered, the 2DES makes an abrupt transition to a fully magnetized state below 2.00; this is signaled by a vanishing of B_M (B–D). At even lower densities, when $n \lesssim 1.70$, the sample turns highly insulating and exhibits nonlinear I - V , suggestive of a pinned Wigner solid. (B) Our experimental technique to measure spin polarization of the 2DES, demonstrated using data taken at $n = 2.63$ and density-of-states diagrams. The sample resistance $R_{[100]}$, measured along the [100] direction (Inset), increases as the magnetic field $B_{||}$ applied parallel to the 2DES plane polarizes the electron spins and then saturates once the system is fully magnetized at the field B_M . Above B_M , the Zeeman energy (E_z) exceeds the Fermi energy (E_F); $g(E)$ is the density of states. (C) Resistance ($R_{[100]}$) vs. $B_{||}$ data taken at different 2DES densities ($R_{[010]}$ data show a similar behavior). Traces are shown for both up- and down-sweeps of $B_{||}$ and are offset vertically. The vertical arrows mark the positions of B_M above which the resistance saturates. They are placed symmetrically with respect to $B_{||} = 0$ and are based on the average of four values of B_M (for up- and down-sweeps and $+B_{||}$ and $-B_{||}$). For $n \leq 2.00$, the traces are flat, and there is no hint of a B_M . (D) B_M and (E) the deduced spin susceptibility plotted as a function of density (lower axis) and r_s (top axis). All measurements were performed at $T = 0.30$ K.

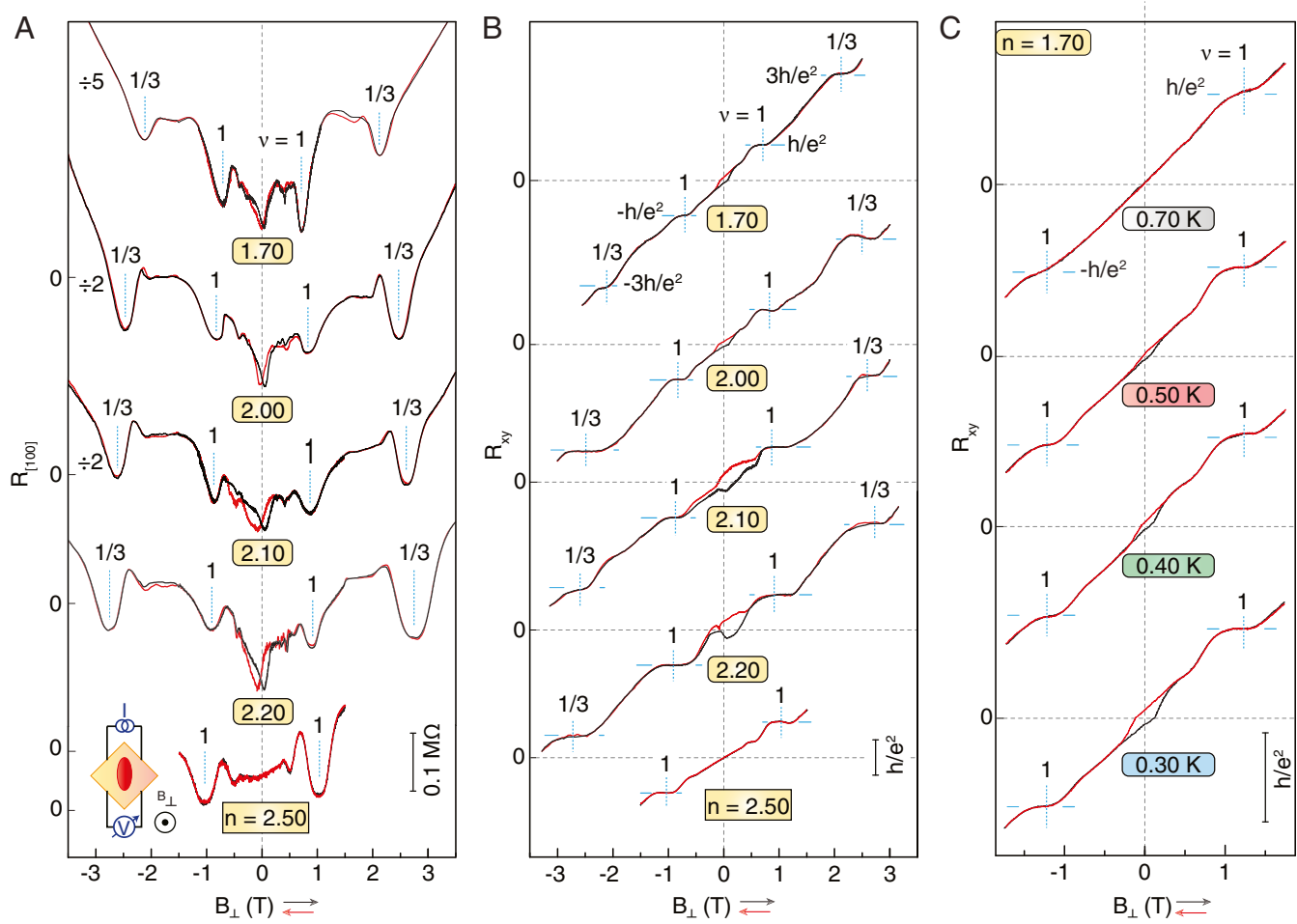


Fig. 2. Magnetotransport data near $n = n_c$. (A) Longitudinal ($R_{[100]}$) and (B) Hall (R_{xy}) resistances, measured at $T = 0.30$ K, shown as a function of perpendicular magnetic field (B_{\perp}) for five densities as indicated (in units of 10^{10} cm^{-2}). As the density is lowered, a pronounced hysteresis near $B_{\perp} = 0$ emerges close to $n_c = 2.00$ and continues at $n < n_c$. The longitudinal resistance traces show deep minima at Landau level filling factors $v = 1$ and $1/3$, accompanied by nearly quantized plateaus in R_{xy} at the expected values, signaling well-developed quantum Hall states at these fillings. The presence of fractional quantum Hall states at densities as low as $n = 1.70$ demonstrates the extremely high quality of the 2DES and the presence of electron–electron interaction. (C) Temperature dependence of R_{xy} , taken at $n = 1.70$, showing that the hysteresis vanishes at high temperatures ($T \simeq 0.70$ K).

Signatures of Spontaneous Ferromagnetism. First, we present data for the case where all of the electrons are transferred to the [010] valley, i.e., the valley whose longer Fermi wave vector axis is along the [010] direction (Fig. 1B, *Bottom, Inset*) (for more details, see *SI Appendix, section I*). We probe the spin polarization via measuring the 2DES resistance as a function of a magnetic field B_{\parallel} applied parallel to the sample plane (Fig. 1B). This is a well-established technique (9, 12–22, 26, 27) whose working principle, as depicted in Fig. 1B, is that the resistance of the 2DES increases as B_{\parallel} polarizes the electrons through the addition of Zeeman energy (E_Z). The partially polarized 2DES has higher resistance because of a reduction in the screening of the disorder potential by the 2D electrons (26, 27). When B_{\parallel} reaches a sufficiently large value (B_M) so that E_Z equals the Fermi energy (E_F), the 2D electrons become fully magnetized, and the resistance no longer rises. Since $E_Z = g\mu_B B$ and $E_F = (2\pi\hbar^2 n)/m$, we have

$$B_M = \left(\frac{2\pi\hbar^2}{\mu_B} \right) \frac{n}{gm}, \quad [1]$$

where g is the band value of the effective Landé g factor and μ_B is the Bohr magneton ($g=2$ in our AlAs 2DES). Note

that B_M is inversely proportional to the product gm which is directly related to the spin susceptibility, χ . In an interacting 2DES, g , m , and χ are typically enhanced by interaction. Denoting the enhanced values by g^* , m^* , and χ^* , one can determine the enhancement factor for the susceptibility $\chi^*/\chi = g^* m^* / gm$ from measuring B_M . In our experiments, we find that as we lower the 2DES density, B_M decreases rapidly, signaling a fast-enhancing χ^*/χ , and then suddenly vanishes below a critical density n_c (Fig. 1C–E). This observation strongly suggests that the 2DES is fully magnetized for $n \leq n_c$ in the absence of an applied magnetic field.

Fig. 1C–E capture the evolution described above. In Fig. 1C we show $R_{[100]}$ vs. B_{\parallel} applied along the [100] direction (Fig. 1B, *Inset*). For $n \geq 2.10$, $R_{[100]}$ rises with B_{\parallel} and saturates above a density-dependent field B_M , marked by vertical arrows in Fig. 1C. As discussed above (Fig. 1B), B_M signals the full magnetization of the 2DES and allows us to deduce the spin susceptibility. In Fig. 1D and E we show plots of the measured B_M and the deduced susceptibility as a function of n . As expected for a dilute, interacting 2DES, when n is lowered, B_M decreases quickly as susceptibility increases (6, 17). The principal finding in our experiments is that as n is lowered below 2.10, the traces in Fig. 1C become completely independent of B_{\parallel} with no sign

of a B_M whatsoever. A most logical interpretation of this behavior is that for $n \leq 2.00$, the 2DES is fully magnetized at $B_{\parallel} = 0$, expected for spontaneous ferromagnetism. The critical density $n_c = 2.00$ corresponds to $r_s = 34.5$.

It is noteworthy in Fig. 1C that the trace taken at a slightly larger density, $n = 2.10$, exhibits a pronounced hysteresis near $B_{\parallel} = 0$. In Fig. 2A and B we show $R_{[100]}$ and R_{xy} (Hall resistance) traces taken as a function of perpendicular magnetic field, B_{\perp} . Hysteretic features near zero magnetic field are clearly visible here too and are most pronounced when n is close to n_c . These features suggest a possible formation of magnetic domains, as expected near a magnetic transition. Notably, as seen in Fig. 2C, the hysteresis vanishes at high temperatures; e.g., at $n = 1.70$, the hysteresis disappears at $T \approx 0.70$ K.

We note that the technique we use to probe the enhancement and divergence of the spin susceptibility is similar to what was used in many previous studies of the spin polarization of dilute 2D carriers (9, 12–22, 26, 27). None of the previous studies, however, reported a sudden and complete disappearance of the magnetoresistance as a function of B_{\parallel} (implying a vanishing B_M and full magnetization) as the 2DES density is reduced below a critical value. In some of these studies, e.g., in the work of ref. 16 on Si/SiO₂, nonzero magnetoresistance was observed down to the lowest achievable densities, and a plot of B_M (deduced from fitting the magnetoresistance to an empirical expression) vs. n was extrapolated to lower densities to conclude that B_M vanishes at a finite density (corresponding to an $r_s \approx 9$). As shown in ref. 17, such extrapolation can be misleading, and recent new measurements (21, 22) indeed conclude that there is no magnetic instability or complete spin polarization at zero magnetic field in the Si/SiO₂ system even at densities lower than those achieved in ref. 16 (see, e.g., point 7 on p. 10 of ref. 21).

We believe it is the exceptionally high sample quality that allows us to explore the interaction phenomena even in the extremely dilute case and observe a spontaneous magnetization. The high quality of our 2DES can be inferred from Fig. 2A and B traces. At Landau level filling factor $\nu = 1$ and $1/3$ ($\nu = nh/eB_{\perp}$), we observe clear indications of integer and fractional quantum Hall states, signaled by resistance minima in $R_{[100]}$ minima and reasonably well-quantized plateaus in R_{xy} even at $n = 1.70$ ($r_s \approx 38$). (We observe $R_{[100]}$ minima at $\nu = 1$ and $1/3$ down to $n = 1.20$ [$r_s \approx 45$].) The observation of fractional quantum Hall states down to such small densities is particularly noteworthy as it attests to the presence of interaction even when the 2DES is extremely dilute.

We would like to highlight two points before closing this section. First, note that Eq. 1 assumes that gm (i.e., the spin susceptibility, χ) is a constant, independent of B_{\parallel} . This assumption is consistent with the conclusions of previous studies (17). While our determination of χ^* relies on this assumption, we emphasize that our main conclusion, namely, that the 2DES undergoes a spontaneous spin polarization below a critical density, is based on the vanishing of B_M and does not depend on such an assumption. Second, as shown in SI Appendix, section IV, the value of $R_{[100]}$ (which is constant and independent of B_{\parallel}) at $n = 2.00$ is close to the saturated value of $R_{[100]}$ at large B_{\parallel} at $n = 2.10$. This observation confirms our conclusion that the 2DES is fully spin polarized at $n = 2.00$ at $B_{\parallel} = 0$, just as it is at $n = 2.10$ at large B_{\parallel} .

Is There a Link between the Spontaneous Ferromagnetism and the MIT? As mentioned in the opening paragraphs, a possible link between the spin polarization and MIT in dilute 2D carrier systems has been debated heavily (9, 11–22). In Fig. 3A we show the temperature dependence of the sample resistance measured at $B = 0$. At the highest n , the behavior is metallic, with resistance

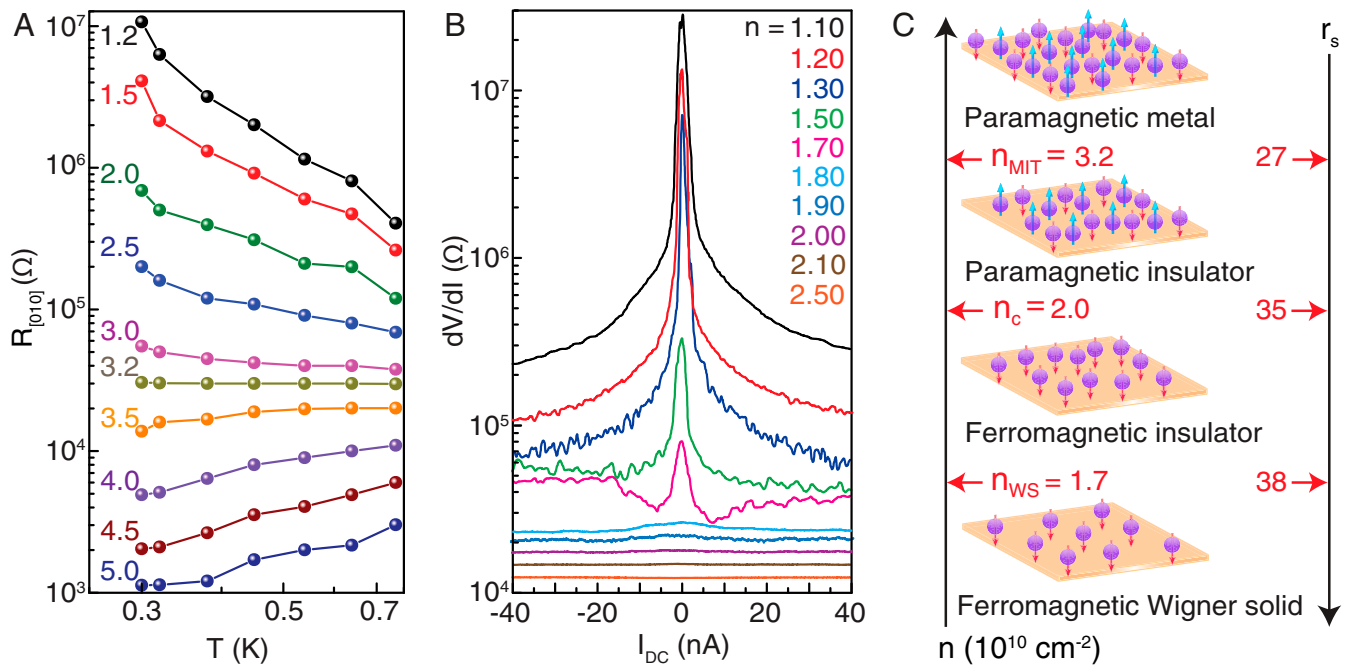


Fig. 3. Summary of temperature-dependent and nonlinear I - V data and the phases that we observe as a function of n (or r_s). (A) $R_{[010]}$, resistance measured along [010], as a function of temperature exhibiting metallic transport for $n \geq 3.2$, and a switch over to an insulating behavior for smaller n . $R_{[100]}$ data show a qualitatively similar behavior. (B) Differential resistance (dV/dI) measured along [100] at $T = 0.30$ K, plotted against the DC bias current, showing increasing nonlinearity at small biases when $n \lesssim 1.70$. (C) Illustration of different phases observed in our 2DES. Starting as a paramagnetic metal at large n (small r_s), the 2DES undergoes a cascade of transitions to a paramagnetic insulator, ferromagnetic insulator, and finally to a ferromagnetic solid as the density is lowered.

decreasing with decreasing temperature, while at the lowest densities, an opposite, insulating behavior is seen. The density at which the behavior switches is $n_{MIT} \approx 3.2$ ($r_s \approx 27$), well above $n_c = 2.0$, the onset of the transition to full magnetization. This is again consistent with the data of ref. 17 but disagrees with the conclusions of ref. 16. It is also noteworthy that $r_s \approx 27$ at which we observe the MIT is much larger than r_s reported in other 2D carrier systems for the MIT, except for very clean GaAs 2D hole systems (10).

We would like to emphasize that while we do not see a link between the MIT and the full magnetization of the 2DES (as inferred from the sudden disappearance of B_M in Fig. 1C data), we do observe certain anomalies in the magnetoresistance traces near $n_{MIT} \approx 3.2$. As seen in Fig. 1C, at $n = 3.30$, just above the MIT, the resistance shows a very rapid rise as a function of B_{\parallel} at very low fields, followed by an unusual linear rise with B_{\parallel} at higher fields before saturation. This behavior is not unique to this trace and can be seen in a range of densities between ≈ 3.60 and

≈ 3.05 , near the MIT (SI Appendix, Fig. S4). Another noteworthy feature is a change in the slope of B_M vs. n plot in Fig. 1D at n_{MIT} : it appears that the B_M drop with lowering the density accelerates below n_{MIT} . A qualitatively similar feature was reported recently for Si/SiO₂ 2DESs (22). We will return to these anomalous features in our interpretation of the data in *Interpretation of the Ferromagnetic Transition*.

Hints of Wigner Solid. In Fig. 3B, we address another fundamental property of our 2DES at very low densities. Fig. 3B displays differential resistance (dV/dI) as a function of applied DC current I_{DC} ; see SI Appendix, sections V–VII, for measurement details and additional data. At densities $n \geq n_c$, dV/dI is linear. As the density is lowered below n_c , I - V slowly becomes nonlinear, and at the lowest densities, it is strongly nonlinear. As demonstrated in SI Appendix, Fig. S11, this nonlinearity is a strong function of temperature and vanishes at high temperatures. Previous studies on extremely dilute 2D carrier systems at $B = 0$

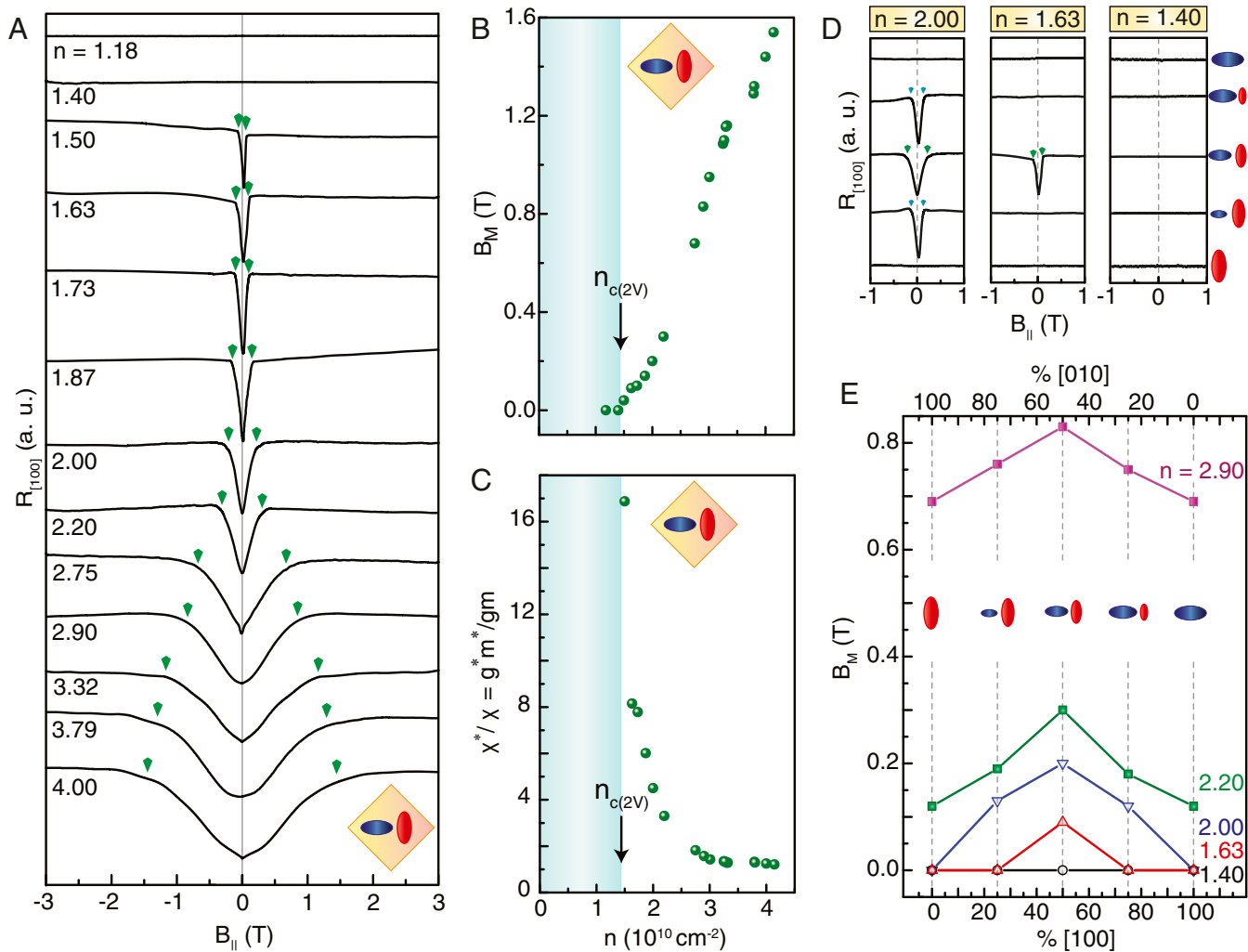


Fig. 4. Controlling the spin polarization and ferromagnetic transition by tuning the valley occupancy. (A) Resistance vs. B_{\parallel} data taken at $T = 0.30$ K for different 2DES densities when the two occupied valleys are degenerate. The vertical arrows mark the positions of B_M . They are placed symmetrically with respect to B_{\parallel} and are based on the average of two values of B_M (for $+B_{\parallel}$ and $-B_{\parallel}$). For $n \leq 1.40$, the traces are flat, and there is no hint of a B_M . (B and C) B_M and the deduced spin susceptibility of the valley-degenerate 2DES plotted as a function of density. (D) Resistance vs. B_{\parallel} data taken at three 2DES densities demonstrating the effect of the valley occupancy on B_M (marked with vertical arrows). The valley occupancy is graphically indicated on the right. At a fixed density, the 2DES has the smallest B_M when only one valley (either [100] or [010]) is occupied. As electrons transfer from one valley to the other, B_M increases and reaches its maximum value when the valleys are equally occupied. The single-valley case reaches the ferromagnetic transition at the largest density, while the valley-degenerate case requires the smallest density. (E) B_M plotted against the valley occupancy, showing a clear increase in B_M as we move from single-valley cases (0 and 100%) toward the valley-degenerate (50%) case.

(10), or at very small Landau level fillings (28), have concluded that the nonlinear I - V suggests the depinning of a Wigner solid which is pinned by the ubiquitous disorder potential. This conclusion has been corroborated by numerous experimental studies, including microwave resonance and other measurements (29–32). It is possible that in our 2DES, too, the nonlinear I - V signals the formation of a pinned Wigner solid at $r_s \gtrsim 38$ ($n \lesssim 1.70$).

An intriguing observation in our experiments is that the fractional quantum Hall states still show up in a density regime where the longitudinal resistance at $B=0$ is extremely large $\gg h/e^2$ and the 2DES exhibits a strongly insulating temperature dependence. The resistance is also extremely large at $\nu=1/3$, but remarkably, its value at $\nu=1/3$ decreases as we lower the temperature, as expected for a fractional quantum Hall liquid state. The notion that a pinned Wigner solid at $B=0$ would make a transition to a correlated liquid state in a perpendicular field might sound counterintuitive but in fact is consistent with conclusions implied by the theoretical work of Zhao et al. (33).

Phase Diagram for an Interacting 2D Electron System. The observations of MIT, spontaneous magnetization, and nonlinear I - V response as a function of n (or r_s) lead us to suggest an experimental phase diagram for the ground states of our interacting 2DES, as highlighted in Fig. 1A. The ground states include four distinct phases as a function of decreasing n (i.e., increasing r_s), as schematically represented in Fig. 3C: 1) paramagnetic metal, 2) paramagnetic insulator, 3) ferromagnetic insulator, and 4) ferromagnetic Wigner solid.

Interpretation of the Ferromagnetic Transition. A simple but possibly naïve interpretation of the observed ferromagnetic transition we observe is that it is a Bloch transition (1). As alluded to in the Introduction, in 1929, Felix Bloch suggested that itinerant electrons should spontaneously magnetize at sufficiently low densities. Our observation of the spontaneous ferromagnetism is highly reminiscent of such a phenomenon. A transition at lower densities to a state that we identify as a Wigner solid would also make qualitative sense in this simple picture. Such a picture is also qualitatively consistent with the Monte Carlo calculations of ref. 6 which were done for a disorder-free 2DES, although there are quantitative discrepancies. For example, the value of r_s ($\simeq 35$) at which we observe the ferromagnetic transition is larger than the value ($\simeq 26$) predicted by ref. 6. So is the value of r_s ($\simeq 38$) above which we see signs of a possible Wigner solid formation (ref. 6 predicts $r_s \simeq 35$). These quantitative discrepancies might come from the fact that the calculations are performed for an ideal 2DES, with no disorder, zero electron layer thickness, and an isotropic effective mass. In our 2DES, on the other hand, the electrons have a nonzero layer thickness and occupy a valley with an anisotropic effective mass. Both the finite electron layer thickness and the mass anisotropy are known to reduce the interaction strength and the enhancement of the spin susceptibility at a given r_s (34) and can move the onset of full magnetization to larger r_s .

However, there is an important caveat. As clean as our sample might be, there is some finite disorder because of the presence of ionized impurities. The disorder is indeed the likely cause for the 2DES exhibiting an insulating behavior below n_{MIT} . On the other hand, our observation of a spontaneous ferromagnetism and the fractional quantum Hall features that we observe at n_c and even lower densities (Fig. 2) provide strong evidence that

interaction is playing a dominant role. An alternative interpretation of our data is then as follows. It has been shown theoretically that a direct first-order transition between a metallic Fermi liquid state and a Wigner solid is forbidden in 2D and that there should be one or more exotic microemulsion phases in an intermediate density range (20, 35). It might be that the ferromagnetic transition we observe is occurring in such a microemulsion phase. The anomalous features seen in the resistance vs. B_{\parallel} data near the MIT (Fig. 1C and *SI Appendix*, Fig. S4) could be manifestations of such exotic intermediate phases. Also, given the anisotropy of the effective mass in our system and that the resistance we measure in this phase is anisotropic ($R_{[100]} < R_{[010]}$), it is possible that the intermediate phase is nematic or smectic as proposed theoretically (20, 35). Moreover, the theory of refs. 35, 36 concludes that the Wigner solid phase stabilized at the lowest densities has ferromagnetic order. This scenario is consistent with our data: we see $B_M=0$ even below $n \simeq 1.70$ where we infer a transition to a pinned Wigner solid phase in our 2DES.

Role of the Valley Degree of Freedom in the Spin Polarization. Another important highlight of experiments is captured in Fig. 4 where we illustrate how the valley polarization impacts the ferromagnetic transition. How we tune the valley occupancy is described in *SI Appendix*, section I. In Fig. 4A we show a plot similar to Fig. 1C except that here the valleys are degenerate. We also show plots of the measured B_M and the deduced spin susceptibility as a function of n in Fig. 4B and C. Qualitatively similar to Fig. 1C–E, when n is lowered, B_M decreases rapidly as susceptibility increases. However, in the valley-degenerate case, the critical density below which B_M vanishes is $n_{c(2V)} = 1.40$ instead of $n_{c(1V)} = 2.00$ of the single-valley-occupied 2DES (Fig. 1 C–E). This finding is consistent with previous measurements (at much higher densities) (37, 38) and theoretical calculations (39) which concluded that the enhancement of the spin susceptibility, at a given density, is smaller for a two-valley system compared to a single-valley one. The phenomenon can be attributed to the modification of the exchange energy in the system because of the extra (valley) degree of freedom.

The tunability of the valley occupancy allows us to investigate the ferromagnetic transition as a function of partial valley occupancy. As shown in Fig. 4 D and E, B_M is largest when the valleys are degenerate. As we lift the degeneracy and move toward valley polarization, B_M starts to drop and eventually attains its smallest value when the electrons are completely valley polarized. This means that the spin susceptibility is maximum when the 2DES is valley polarized and minimum when the valleys are degenerate, for a given density. Thanks to this interplay between the spin and valley degrees of freedom, we can control the onset of the ferromagnetic transition via tuning the valley occupancy, opening up exciting avenues to integrate spintronics and valleytronics in the same device.

Data Availability. All study data are available in the main text and *SI Appendix*.

ACKNOWLEDGMENTS. We acknowledge support through the US Department of Energy Basic Energy Science (Grant DEFG02-00-ER45841) for measurements, the National Science Foundation (Grants DMR 1709076, ECCS 1906253, and MRSEC DMR 1420541), and the Gordon and Betty Moore Foundation's Emergent Phenomena in Quantum Systems Initiative (Grant GBMF9615 to L.N.P.) for sample fabrication and characterization. We also thank D. M. Ceperley, H. D. Drew, J. K. Jain, S. A. Kivelson, M. A. Mueed, and M. P. Sarachik for illuminating discussions.

1. F. Bloch, Bemerkung zur Elektronentheorie des Ferromagnetismus und der elektrischen Leitfähigkeit. *Z. Phys.* **57**, 545–555 (1929).
2. E. Wigner, On the interaction of electrons in metals. *Phys. Rev.* **46**, 1002–1011 (1934).
3. E. C. Stoner, Ferromagnetism. *Rep. Prog. Phys.* **11**, 43–112 (1947).
4. N. W. Ashcroft, N. D. Mermin, *Solid State Physics*, (Saunders, Philadelphia, 1976), p. 682.
5. B. Tanatar, D. M. Ceperley, Ground state of the two-dimensional electron gas. *Phys. Rev. B* **39**, 5005–5016 (1989).
6. C. Attaccalite, S. Moroni, P. Gori-Giorgi, G. B. Bachelet, Correlation energy and spin polarization in the 2D electron gas. *Phys. Rev. Lett.* **88**, 256601 (2002).
7. N. D. Drummond, R. J. Needs, Phase diagram of the low-density two-dimensional homogeneous electron gas. *Phys. Rev. Lett.* **102**, 126402 (2009).

8. T. Sajoto, Y. W. Suen, L. W. Engel, M. B. Santos, M. Shayegan, Fractional quantum Hall effect in very-low-density GaAs/Al_xGa_{1-x}As heterostructures. *Phys. Rev. B* **41**, 8449–8460 (1990).
9. J. Zhu, H. L. Stormer, L. N. Pfeiffer, K. W. Baldwin, K. W. West, Spin susceptibility of an ultra-low-density two-dimensional electron system. *Phys. Rev. Lett.* **90**, 056805 (2003).
10. J. Yoon, C. C. Li, D. Shahar, D. C. Tsui, M. Shayegan, Wigner crystallization and metal-insulator transition of two-dimensional holes in GaAs at $B = 0$. *Phys. Rev. Lett.* **82**, 1744–1747 (1999).
11. S. J. Papadakis, E. P. De Poortere, H. C. Manoharan, M. Shayegan, R. Winkler, The effect of spin splitting on the metallic behavior of a two-dimensional system. *Science* **283**, 2056–2058 (1999).
12. E. Tutuc, E. P. De Poortere, S. J. Papadakis, M. Shayegan, In-plane magnetic field induced spin polarization and transition to insulating behavior in two-dimensional hole systems. *Phys. Rev. Lett.* **86**, 2858–2861 (2001).
13. R. Winkler et al., Anomalous spin polarization of GaAs two-dimensional hole systems. *Phys. Rev. B* **72**, 195321 (2005).
14. T. Okamoto, K. Hosoya, S. Kawaji, A. Yagi, Spin degree of freedom in a two-dimensional electron liquid. *Phys. Rev. Lett.* **82**, 3875–3878 (1999).
15. S. A. Vitkalov, H. Zheng, K. M. Mertes, M. P. Sarachik, T. M. Klapwijk, Scaling of the magnetoconductivity of silicon MOSFETs: Evidence for a quantum phase transition in two dimensions. *Phys. Rev. Lett.* **87**, 086401 (2001).
16. A. A. Shashkin, S. V. Kravchenko, V. T. Dolgopolov, T. M. Klapwijk, Indication of the ferromagnetic instability in a dilute two-dimensional electron system. *Phys. Rev. Lett.* **87**, 086801 (2001).
17. K. Vakili, Y. P. Shkolnikov, E. Tutuc, E. P. De Poortere, M. Shayegan, Spin susceptibility of two-dimensional electrons in narrow AlAs quantum wells. *Phys. Rev. Lett.* **92**, 226401 (2004).
18. O. Gunawan et al., Spin-valley phase diagram of the two-dimensional metal-insulator transition. *Nat. Phys.* **3**, 388–391 (2007).
19. S. V. Kravchenko, M. P. Sarachik, Metal-insulator transition in two-dimensional electron systems. *Rep. Prog. Phys.* **67**, 1–44 (2004).
20. B. Spivak, S. V. Kravchenko, S. A. Kivelson, X. P. A. Gao, Colloquium: Transport in strongly correlated two-dimensional electron fluids. *Rev. Mod. Phys.* **82**, 1743–1766 (2010).
21. V. M. Pudalov, A. Y. Kutsevich, M. E. Gershenson, I. S. Burmistrov, M. Reznikov, Probing spin susceptibility of a correlated two-dimensional electron system by transport and magnetization measurements. *Phys. Rev. B* **98**, 155109 (2018).
22. S. Li, Q. Zhang, P. Ghaemi, M. P. Sarachik, Evidence for mixed phases and percolation at the metal-insulator transition in two dimensions. *Phys. Rev. B* **99**, 155302 (2019).
23. J. Falson, M. Kawasaki, A review of the quantum Hall effects in MgZnO/ZnO heterostructures. *Rep. Prog. Phys.* **81**, 056501 (2018).
24. Y. J. Chung et al., Multivalley two-dimensional electron system in an AlAs quantum well with mobility exceeding $2 \times 10^9 \text{ cm}^2/\text{Vs}$. *Phys. Rev. Materials* **2**, 071001 (2018).
25. M. Shayegan et al., Two-dimensional electrons occupying multiple valleys in AlAs. *Phys. Status Solidi* **243**, 3629–3642 (2006).
26. V. T. Dolgopolov, A. Gold, Magnetoresistance of a two-dimensional electron gas in a parallel magnetic field. *JETP Lett.* **71**, 27–30 (2000).
27. I. F. Herbut, The effect of parallel magnetic field on the Boltzmann conductivity and the Hall coefficient of a disordered two-dimensional Fermi liquid. *Phys. Rev. B* **63**, 113102 (2001).
28. V. J. Goldman, M. Santos, M. Shayegan, J. E. Cunningham, Evidence for two-dimensional quantum Wigner crystal. *Phys. Rev. Lett.* **65**, 2189–2192 (1990).
29. F. I. B. Williams et al., Conduction threshold and pinning frequency of magnetically induced wigner solid. *Phys. Rev. Lett.* **66**, 3285–3288 (1991).
30. Y. Chen et al., Melting of a 2D quantum electron solid in high magnetic field. *Nat. Phys.* **2**, 452–455 (2006).
31. L. Tiemann, T. Rhone, N. Shibata, K. Muraki, NMR profiling of quantum electron solids in high magnetic fields. *Nat. Phys.* **10**, 648–652 (2014).
32. H. Deng et al., Commensurability oscillations of composite fermions induced by the periodic potential of a wigner crystal. *Phys. Rev. Lett.* **117**, 096601 (2016).
33. J. Zhao, Y. Zhang, J. K. Jain, Crystallization in the fractional quantum Hall regime induced by Landau-level mixing. *Phys. Rev. Lett.* **121**, 116802 (2018).
34. T. Gokmen et al., Spin susceptibility of interacting two-dimensional electrons with anisotropic effective mass. *Phys. Rev. B* **76**, 233301 (2007).
35. B. Spivak, S. A. Kivelson, Phases intermediate between a two-dimensional electron liquid and Wigner crystal. *Phys. Rev. B* **70**, 155114 (2004).
36. S. Chakravarty, S. Kivelson, C. Nayak, K. Voelker, Wigner glass, spin liquids and the metal-insulator transition. *Philos. Mag.* **B79**, 859–868 (1999).
37. Y. P. Shkolnikov, K. Vakili, E. P. De Poortere, M. Shayegan, Dependence of spin susceptibility of a two-dimensional electron system on the valley degree of freedom. *Phys. Rev. Lett.* **92**, 246804 (2004).
38. T. Gokmen, M. Padmanabhan, M. Shayegan, Contrast between spin and valley degrees of freedom. *Phys. Rev. B* **81**, 235305 (2010).
39. M. Marchi, S. D. Palo, S. Moroni, G. Senatore, Correlation energy and the spin susceptibility of the two-valley two-dimensional electron gas. *Phys. Rev. B* **80**, 035103 (2009).